ACS OMEGA

Open Access

http://pubs.acs.org/journal/acsodf

Article

Phosphorodiamidate Morpholino Oligomers-Loaded Nanobubbles for Ultrasound-Mediated Delivery to the Myocardium in Muscular Dystrophy

Yoko Endo-Takahashi,[#] Akane Sakurai,[#] Yukiko Oguri,[#] Fumihiko Katagiri, Saki Akiyama, Sanae Sashida, Taiki Yamaguchi, Tetsuro Marunouchi, Ryo Suzuki, Kazuo Maruyama, Kouichi Tanonaka, Motoyoshi Nomizu, and Yoichi Negishi*

Cite This: *ACS Omega* 2025, 10, 9639−9648

Read Online

ACCESS | Metrics & More | Article Recommendations | Supporting Information

ABSTRACT: Microbubbles (MBs) and nanobubbles (NBs) can oscillate and collapse in response to ultrasound exposure, resulting in contrast and delivery effects. Therefore, the retention of the entrapped gas is an important condition in bubble formulations, especially for MBs and NBs with lipid shells, and the stability of the lipid membrane is considered to be affected. We previously developed NBs, which are polyethylene glycol-modified liposomes entrapping an ultrasound contrast gas that can serve as nucleic acid carriers and ultrasound contrast agents. In particular, NBs containing cationic lipids were useful as systemic delivery tools that can load genes and nucleic acids on their surfaces. However, the gas retention of NBs containing cationic lipids were low, leaving room for improvement as ultrasound contrast agents. In this study, we attempted to prepare NBs containing anionic lipids to improve their stability in vivo, and found that they lasted longer in contrast time than previous NBs. In order to utilize anionic NBs, we evaluated their usefulness as systemic delivery tools for cationic-peptide-conjugated phosphorodiamidate morpholino oligomers (PMO). PMO has attracted attention as a therapeutic agent for Duchenne muscular dystrophy (DMD); however, its charge neutrality makes its delivery into muscle fibers challenging, especially more difficult to apply PMO to myocardial damage. We examined the systemic delivery of PMO to the heart using a combination of anionic NBs and ultrasound. Furthermore, we evaluated the usability of octaarginine (R8), a cationic cell-penetrating peptide (CPP), in loading PMO onto the surface of NBs and verified the potential of PMO-loaded NBs as a therapy for cardiac dysfunction in muscular dystrophy.

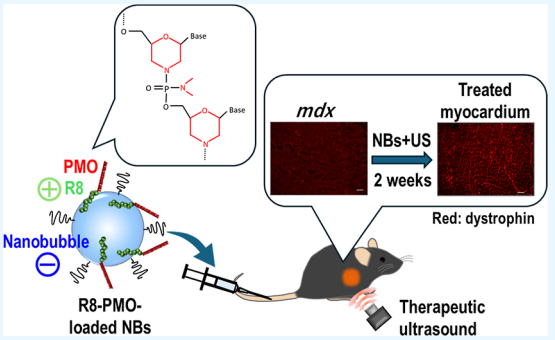

1. INTRODUCTION

Ultrasound-responsive drug delivery systems are expected to be noninvasive and site-specific and have been actively investigated for application involving various modalities, such as small molecules, pDNA, siRNA, miRNA, mRNA, and adeno-associated virus (AAV).[1−10] The use of microbubbles (MBs), which are ultrasound contrast agents, in combination with ultrasound can easily induce the oscillation and cavitation of bubbles.[11−14] It has been found that not only the ultrasound imaging effect but also the drug delivery effect is enhanced by these physical phenomena. Most MBs, including the approved ultrasound contrast agents, are composed of hydrophobic gases and a shell of lipids, polymers, proteins, or surfactants. Nanobubbles (NBs) are also being developed with the potential to reach deep tissues, and most of their compositions are similar to those of MBs. In lipid-based MBs and NBs, it has been reported that the composition and ratio of lipids have a significant impact on gas retention capacity.[15,16]

We previously developed lipid-based NBs that function as ultrasound contrast agents and delivery tools for genes or nucleic acids.[17−23] Particularly, NBs containing cationic lipids can load genes and nucleic acids onto their surfaces, enabling efficient delivery during systemic administration.[24−27] However, NBs with cationic lipids tended to be unstable because of their low gas retention capacity compared with neutral NBs, although there were differences depending on the lipid composition and ratio.[26] The gas retention capacity has a significant effect on the contrast and delivery effects resulting from cavitation. For accurate diagnosis and high therapeutic efficacy, it is necessary for an appropriate amount of NBs to

Received: December 2, 2024
Revised: February 6, 2025
Accepted: February 12, 2025
Published: February 27, 2025

circulate for sufficient time. MBs containing anionic lipids have been reported to stabilize and maintain the ultrasound contrast effects.[15,28] In this study, to improve the gas retention capacity of NBs, we prepared NBs with anionic lipids and examined their physical properties and imaging abilities when combined with ultrasound. It is thought that the preparation of anionic NBs with high stability will improve their usefulness not only as ultrasound contrast agents but also as systemic delivery tools. Therefore, to evaluate the usability of anionic NBs for systemic delivery, we attempted to load cationic peptide-conjugated phosphorodiamidate morpholino oligomers (PMO) onto the surface of NBs. PMO are neutral antisense nucleotides that have attracted attention as therapeutic agents against Duchenne muscular dystrophy (DMD). DMD is considered the most common severe form of muscular dystrophy. It is a muscle disease in which mutations in the X chromosome DMD gene encoding the dystrophin protein result in the loss of its expression.[29] We also reported that the delivery of PMO by ultrasound-responsive NBs may provide an effective treatment method for the lower-limb muscles in DMD.[23,30,31] Several PMOs have been shown to skip exons to allow functional dystrophin expression.[32] However, these effects are primarily observed in skeletal muscles and are difficult to achieve in the myocardium. This is because delivery of PMO to the myocardium is challenging.[33] In addition to reaching the heart stably, PMO must be transfected into the myocardial cells under the strong mechanical forces of beating and blood flow. We examined the systemic delivery of PMO to the heart using the combination of anionic NBs and ultrasound. Furthermore, we evaluated the usability of octaarginine (R8), a cationic cell-penetrating peptide (CPP),[34,35] in loading PMO onto the surface of NBs and verified the potential of PMO-loaded NBs as a treatment for muscular dystrophy.

2. MATERIALS AND METHODS

2.1. Materials. Lipids, 1,2-dipalmitoyl-*sn*-glycero-3-phosphocholine (DPPC), 1,2-distearoyl-*sn*-glycero-3-phosphatidylcholine (DSPC), and *N*-(carbonyl-methoxypolyethylene glycol 2000)-1,2-distearoyl-*sn*-glycero-3-phosphoethanolamine (DSPE-PEG_{2000}), were purchased from NOF Corporation (Tokyo, Japan). Anionic lipid, 1,2-dipalmitoyl-*sn*-glycero-3-phospho-(1′-rac-glycerol) (DPPG) was purchased from Avanti Polar Lipids (Alabaster, AL, USA). Perfluoropropane gas was obtained from Takachiho Chemical Inc. Co. Ltd. (Tokyo, Japan). Phosphorodiamidate morpholino oligomers (PMOs) M23D (+7-18:5′-GGCCAAACCTCGGCTTACCTGAAAT-3′) and 3′-carboxyfluorescein-labeled PMOs were purchased from Gene Tools (Philomath, OR, USA).

2.2. Animals. C57BL/10_{ScSn}*mdx* mice (*mdx* mice) carrying a nonsense mutation in exon 23 of dystrophin were purchased from Japan SLC, Inc. (Shizuoka, Japan). Normal C57BL/6 mice (5 weeks old) were purchased from Tokyo Laboratory Animals Science Co., Ltd. (Tokyo, Japan). All animal experiments and relevant experimental procedures were approved by the Tokyo University School of Pharmacy and Life Sciences Committee on the Care and Use of Laboratory Animals.

2.3. Liposomes to Form NBs. Anionic liposomes were prepared using the reverse-phase evaporation method as described previously.[36] DPPC and PEG_{2000} were dissolved in chloroform. DPPG was dissolved in chloroform, methanol, and HEPES-buffered saline (HBS; 150 mM NaCl, 10 mM HEPES, pH 7.0) (60:30:5 v/v/v). Lipids were mixed at various ratios in chloroform, diisopropyl ether, and HBS (1:1:1 v/v/v), sonicated, and then evaporated. The organic solvent was completely removed, and the size of the liposomes was adjusted to less than 200 nm using extrusion equipment and a sizing filter (Whatman Plc., Kent, UK). After sizing, the liposomes were filter-sterilized using a 0.45 μm syringe filter (Asahi Techno Glass Co., Chiba, Japan). Liposome concentration was determined using a phosphorus assay based on the Fiske protocol.[37] A calibration curve was established on KH_2PO_4 aqueous solutions with concentrations ranging from 0 to 4 mM. For ashing, the liposome suspension was mixed with perchloric acid and nitric acid and incubated at 200 °C for 1 h. After cooling down to room temperature, ammonium molybdate tetrahydrate aqueous solution, hydrochloric acid solution, and freshly prepared ascorbic acid solution were added. The tubes were then plunged into water bath at 60 °C for 2.5 min before reading the absorbance at 820 nm. This assay is on the fact that inorganic phosphate derived from degradation of phospholipids forms a complex with ammonium molybdate that is then reduced by ascorbic acid to provide a colored compound.

To form NBs, 2 mL sterilized vials containing 0.8 mL liposome suspension (total lipid concentration: 1 mg/mL) were filled with perfluoropropane gas, capped, and pressurized with 3 mL of perfluoropropane gas. The vials were placed in a bath sonicator (40 kHz, Bransonic M2800; Branson Ultrasonics Co., Danbury, CT, USA) for 5 min. The zeta potential and mean size of the liposomes and NBs were determined using a light-scattering method with a zeta potential/particle sizer (Nicomp 380ZLS, Santa Barbara, CA, USA).

2.4. Ultrasound Imaging. NBs (total lipid concentration: 1 mg/mL, 100 μL) diluted in HBS (8 mL) were dispensed into 6-well plates. B-mode recordings were performed using a high-frequency ultrasound imaging system (50 MHz, NP60R-UBM; Nepa Gene Co., Ltd., Chiba, Japan).

For in vivo experiments, male ICR mice were anesthetized and injected with NB solution in HBS into the tail vein. Examination of the heart was performed using an Aplio80 ultrasound diagnostic machine (Canon Medical Systems, Tokyo, Japan) and a 12 MHz wideband transducer with contrast harmonic imaging at a mechanical index of 0.27. The mean intensities at various time points after injection into the ROI (region of interest) was quantified.

2.5. PMO Loading onto the Surface of NBs. The R8 peptides and PMO were conjugated using the bifunctional cross-linker, *N*-(6-maleimidocaproyloxy)succinimide. The PMO with primary amine at the 5′ end was reacted with the cross-linker and subsequently with an R8 peptide to form an R8 modified PMO (R8-PMO). To prepare R8-PMO-loaded NBs, adequate amounts of R8-PMO were added to the NBs and gently mixed. FITC-labeled R8-PMO (R8-PMO-FITC) and flow cytometry were used to examine the interaction between R8-PMO and NBs. PMO-FITC without R8 and neutral NBs were also used to evaluate the electrostatic interactions in PMO loading onto the surface of NBs. The fluorescence intensity of the R8-PMO-NBs was analyzed using FACSCanto (Becton Dickinson, San Jose, CA, USA).

2.6. PMO Delivery to the Heart of *mdx* Mice. To evaluate the delivery of PMO into the cardiac tissues of *mdx* mice, a 200 μL solution of R8-PMO-loaded NBs (PMO 100 μg/60 μL, NBs 140 μg lipid/140 μL) was injected into the tail vein of *mdx* mice (5−6 weeks old, male), and the hearts were

https://doi.org/10.1021/acsomega.4c10896
ACS Omega 2025, 10, 9639−9648

Table 1. Physical Properties of Liposomes and NBs

	particle size (nm)		zeta potential (mV)	
DPPC/DPPG/PEG	liposomes	NBs	liposomes	NBs
94:0:6	154.7 ± 44.6	648.1 ± 73.3	−0.40 ± 0.35	0.16 ± 0.50
64:30:6	141.6 ± 47.4	651.6 ± 73.0	−0.96 ± 0.83	−0.27 ± 0.27
44:50:6	142.9 ± 45.2	644.7 ± 73.3	−0.53 ± 1.08	−0.51 ± 0.38
0:94:6	126.0 ± 54.8	594.6 ± 82.6	−0.46 ± 0.06	−0.42 ± 0.58

immediately exposed to ultrasound irradiation (frequency, 1 MHz; duty, 50%; intensity, 2 W/cm^2; time, 60 s). Sonitron 2000 (NEPA GENE Co., Ltd. Chiba, Japan) was used as ultrasound generator. For comparison, groups treated with a mixture of NBs and PMO without R8 were also processed under the same conditions. Two weeks after injection, the heart was collected and embedded in an OCT compound, and immediately frozen at −80 °C. Serial sections 6 μm thick were cut using a cryostat. Sections were stained with an NCL-DYS2 monoclonal antibody that strongly reacts with the C-terminal region of dystrophin. Alexa Fluor 546 (Thermo Fisher Scientific Inc., MA, USA) was used as the secondary antibody. Each section was observed under a fluorescence microscope (KEYENCE, BZ8100). For dystrophin-positive fiber counting, the maximum number of dystrophin-positive fibers in one section was counted using a fluorescence microscope. Myofibers were considered dystrophin-positive if more than two-thirds of single myofibers showed continuous staining.[38]

2.7. Echocardiographic Measurements. Transthoracic echocardiography was performed on PMO-injected and ultrasound-exposed mice according to a previously described method.[39] Normal C57BL/6 or *mdx* mice were immobilized with 30 mg/kg i.p. injected sodium thiopental, and their chest hair was shaved off before examination. During the measurements of cardiac parameters, the body temperature of mice was kept at 37 °C on a heated mat. Two-dimensional and Doppler imaging were performed by using a ProSound 5500 (Aloka, Tokyo, Japan) equipped with a 13 MHz transducer. A transthoracic echocardiographic probe was used to obtain the short- and long-axis views. The left ventricular internal diameters at end-diastole and systole were measured, and left ventricular fractional shortening (FS) and ejection fraction (EF) were calculated from the left ventricular dimensions.

2.8. Creatine Kinase Measurement. Blood was collected through a small cut at the end of the tail 1, 2, 6, 10, and 24 h after the injection of PMO. Creatine kinase levels were analyzed in a clinical pathology laboratory (Oriental Yeast Co., Ltd., Tokyo, Japan).

2.9. Statistics. All data are presented as the mean ± SD (n = 3−4). Data were considered statistically significant at P < 0.05. Two-way ANOVA or Student's t-test was used to calculate statistical significance.

3. RESULTS

3.1. Physical Properties of Anionic NBs. We first examined the effect of anionic lipids on the physical properties of the NBs. Liposomes were prepared by varying the composition ratio of the anionic lipid DPPG and then filled with perfluoropropane gas to form NBs. The particle size and zeta potential were evaluated. Although the particle sizes of liposomes containing DPPG were slightly smaller than those of liposomes without DPPG, the particle sizes of the NBs were similar for all compositions. The zeta potential in the preparation solvent did not change significantly for any composition of liposomes and NBs, regardless of the DPPG content (Table 1 and Figure S1). We then compared the ability of the NBs to retain ultrasonic gas. The contrast images showed similar levels of brightness regardless of the anionic lipid content (Figure 1A). No remarkable differences in the intensity or the persistence were also observed when the brightness of the region of interest (ROI) was quantified (Figure 1B).

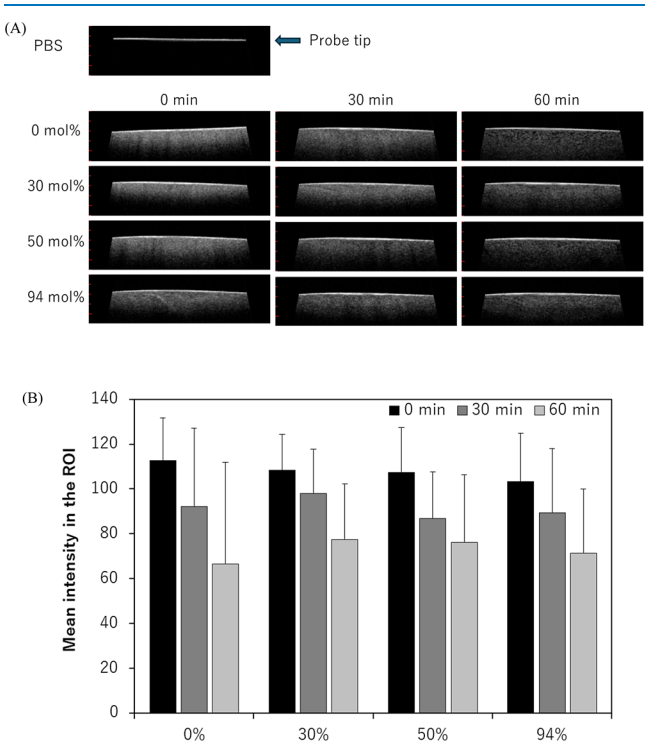

Figure 1. Ultrasound contrast effects of NBs containing anionic lipid. (A) Ultrasonographic images of NBs in the well plate was obtained by NP60R-UBM and its probe (50 MHz). (B) The mean intensity of pixels in the ROI (region of interest) was quantified.

3.2. Ultrasound Imaging Ability of NBs Containing Anionic Lipid. To investigate the usability of the NBs containing anionic lipids as ultrasound contrast agents, we compared their ultrasound imaging capabilities with those of our previously developed NBs without anionic lipids. When a diagnostic ultrasound probe was applied to the heart after NBs were administered via the tail vein, the contrast intensity of the NBs containing anionic lipids persisted for a longer period, as shown in Figure 2. This result suggests that NBs containing anionic lipids can stably retain gas in vivo.

3.3. Loading of R8-PMO onto the Surface of Anionic NBs. NBs containing anionic lipids have the potential to become useful carriers by loading cationic materials onto their surfaces. To verify this possibility, we added fluorescently labeled octa-arginine peptide-conjugated PMO (R8-PMO) to

https://doi.org/10.1021/acsomega.4c10896
ACS Omega 2025, 10, 9639−9648

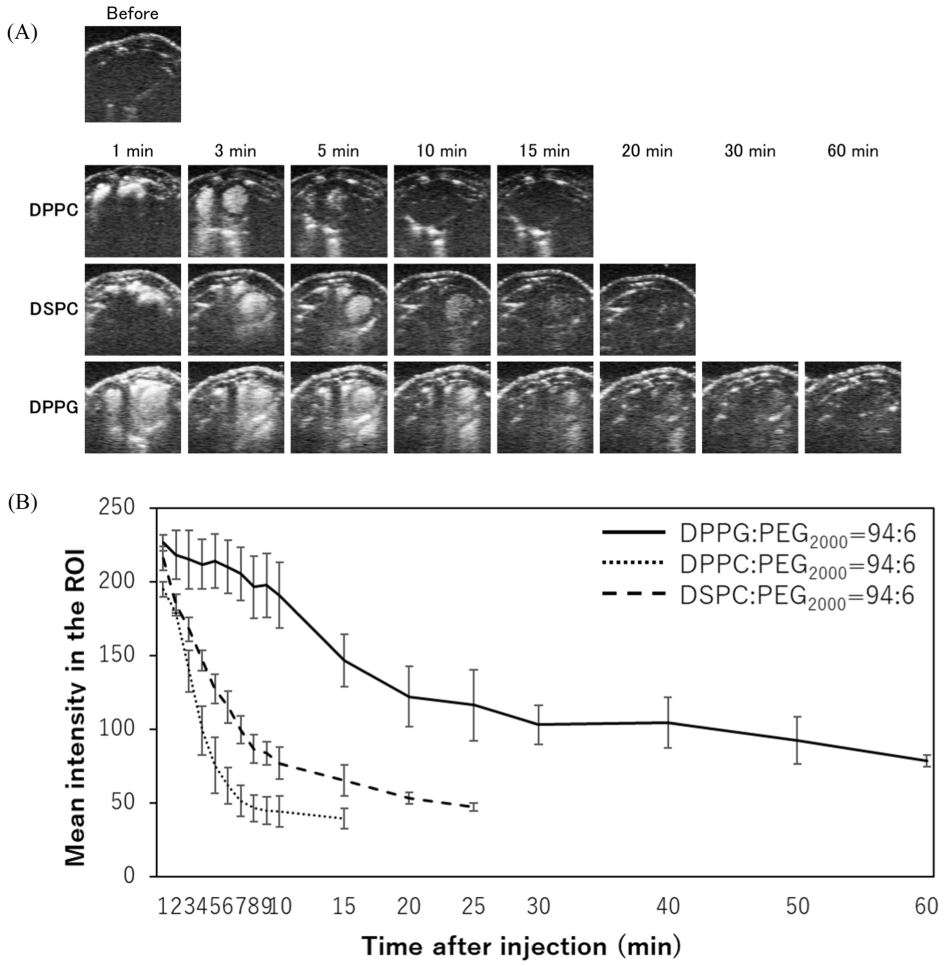

Figure 2. The effects of lipid composing NBs on ultra-sonographic imaging in vivo. (A) Ultra-sonographic images of the heart was obtained by Aplio and its probe (12 MHz). (B) The mean intensity of pixels in the ROI (region of interest) was quantified.

the NBs and analyzed the interaction by flow cytometry. The analysis by flow cytometry could be utilized as a simplified assessment of the interactions, because fluorescently labeled PMOs are too small to be detected by flow cytometry and become detectable when loaded onto NBs. As shown in Figure 3A, the interaction between PMO and NBs was significantly increased by the combination of R8-PMO and anionic NBs. These results suggested that R8-PMO could be loaded onto anionic NBs by electrostatic interaction. The interaction between NBs and R8-PMO increased in a dose-dependent manner following the addition of R8-PMO. The upper limit of the interaction was suggested to be approximately 400 pmol of R8-PMO for 60 μg of NBs, and no significant changes were observed in the physical properties of the NBs (Figures 3B, S2, and Table 2).

3.4. PMO Delivery to the Heart by the Combination with R8-PMO-Loaded NBs and Ultrasound. We attempted to deliver PMO or R8-PMO to the heart using a combination of ultrasound and NBs and evaluated dystrophin expression following PMO transfection using immunohistochemistry. As shown in Figure 4A, dystrophin expression in heart sections was restored by treatment with R8-PMO compared to that with PMO, even when neutral NBs were used. The effect was enhanced in the group treated with R8-PMO-loaded NBs rather than with a mixed solution of neutral NBs. Quantitative evaluation of the number of dystrophin-positive fibers showed that the number of positive fibers significantly increased in the group treated with R8-PMO-loaded anionic NBs in combination with ultrasound exposure to the heart (Figure 4B). In addition, echocardiographic and biochemical studies showed that these treatments were safe in normal and DMD model mice, with no adverse effects on cardiac function before or after the treatments (Figure 4C−E).

4. DISCUSSION

We previously developed NBs with lipid shells and demonstrated their usefulness as gene and nucleic acid delivery and contrast agents.[17−23] In particular, NBs containing cationic lipids that can load pDNA and nucleic acids have been effective for systemic delivery through microvessels.[24−27] However, there are challenges in sustaining the ultrasound contrast gas retention. Previously, it has been reported that the inclusion of small proportions of anionic lipids, such as DPPA (1,2-dipalmitoyl-*sn*-glycero-3-phosphate) and DPPG (1,2-dipalmitoyl-*sn*-glycero-3-phospho-(1′-rac-glycerol)), can reduce coalescence due to the associated electrostatic repulsion between bubbles, resulting in stabilization of the bubbles.[15,28,40] Additionally, it has been reported that addition of phosphatidylglycerol (PG) to lipid membranes composed of phosphatidylcholine (PC) increases the phase transition temperature and stabilizes the membranes.[41] Reports on the stabilization of phospholipid bilayers and the lipid composition of liposomes may be helpful in bubble formulations with lipid

https://doi.org/10.1021/acsomega.4c10896
ACS Omega 2025, 10, 9639−9648

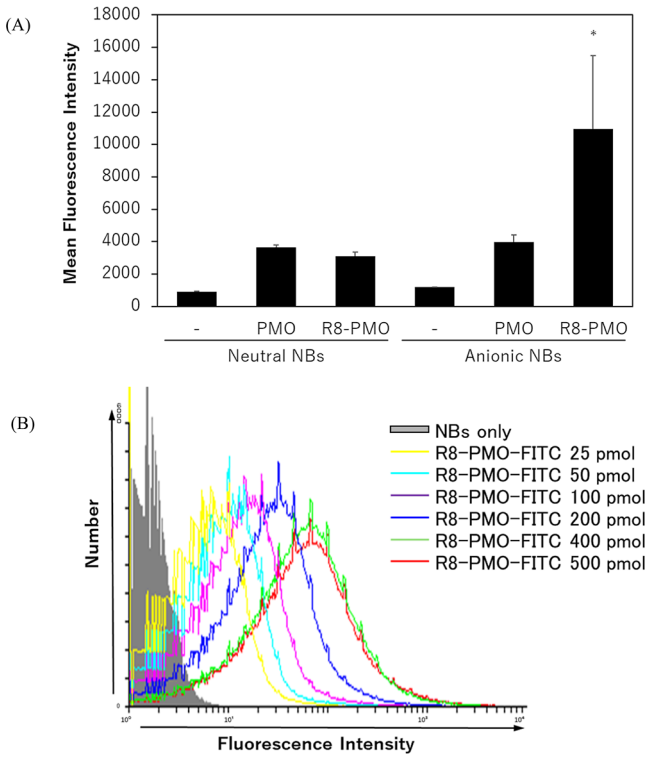

Figure 3. Interaction between R8-PMO and NBs containing anionic lipid. (A) The influence of electrostatic interactions in PMO loading on NBs surfaces. PMO or R8-PMO (100 pmol) was added to NBs (60 μg) containing 94 mol % DPPC or DPPG. Mean fluorescence intensity was analyzed by flow cytometry. The bars show the mean and SD (n = 3). * indicates $P < 0.01$ using a two-way ANOVA with Tukey's posthoc test. (B) FITC-labeled R8-PMO (0−500 pmol) was added to NBs (60 μg) containing 94 mol % DPPG and the interaction was analyzed by flow cytometry.

shells. In fact, it is useful to refer to the information in the case of liposomes to determine the components of lipids in the preparation of NBs containing cationic lipids.[26] Furthermore, MBs containing PC and PG have been reported to show higher stability and blood retention than the approved contrast agents, Sonazoid and SonoVue.[42,43] In this study, NBs containing DPPG, an anionic lipid, were prepared to improve their stability in vivo.

When comparing the contrast brightness of the NBs solutions in the well plates, no significant changes due to PG content were observed (Figure 1). We employed NBs with a higher DPPG content because our goal was not only to improve stability but also to load cationic molecules. The in vivo ultrasound contrast effect of anionic lipid-containing NBs was more persistent than that of neutral lipid-only NBs, which were more stable than cationic lipid-containing NBs (Figure 2). These results indicated that we successfully created stable NBs in vivo, which was one of our objectives. We then attempted to load R8-PMO onto the surface of the anionic lipid-containing NBs. Using flow cytometry, R8-PMO-FITC alone was too small to be detected, and NBs alone were detected, but their fluorescence intensity is low. Only R8-PMO-FITC-loaded NBs were detected with high fluorescence intensity. These results suggest that R8-PMO interacts with the surfaces of anionic NBs. PMOs are chemically modified DNA derivatives in which the deoxyribose pentose sugar units are replaced by morpholine rings and phosphates with a neutral phosphorodiamidate linkage.[44] PMOs exhibit a binding affinity for RNA similar to that of DNA, and efficiently interfere with gene expression in a sequence-specific manner. Their nonionic character, combined with their resistance to degradation, offers efficacy with minimal toxicity.[45] However, the main weakness of this approach is the low efficiency of delivering charge-neutral PMO to the muscle fibers. There have been several reports of PMO conjugated with CPP to address this issue for the treatment of DMD.[46−48] We previously achieved efficient delivery of neutral PMO to hind limb muscles using a combination of NBs and the physical energy of ultrasound.[23,30,31] These reports were targeted to the hind limb muscles via administration into the tibialis anterior muscle or vein of the hind limb. The sites of administration and irradiation were close to each other, which may have allowed for efficient delivery. In the treatment of myocardial damage observed in advanced DMD, it is important to deliver PMO to the heart; systemic administration may be less invasive and more useful than direct myocardial administration. Although PMO is a stable nucleic acid in vivo, its presence with the NB, which is the driving force for transfection, is expected to enhance transfection efficiency after systemic administration. In this study, we used R8-PMO to load neutral PMO onto stable anionic NBs for efficient delivery to the heart and to further improve the transfection efficiency of PMO into myofibers. The combination of NBs and ultrasound improved the delivery efficiency of PMO at doses that were ineffective with PMO alone, further enhancing the efficiency of R8-PMO (Figure 4). Comparison of the results of PMO and R8-PMO delivery by neutral NBs and ultrasound suggested that the presence of R8, which is a CPP, increased the transfection efficiency of PMO into the myocardium. Furthermore, a comparison of neutral NBs and NBs containing anionic lipids revealed a marked enhancement in dystrophin expression in the myocardium. These results indicated that loading PMO onto NBs using R8 is useful for systemic administration. Conventionally, the loading of nucleic acids onto NBs also aims to improve the in vivo stability of nucleic acids. However, as mentioned above, PMO is a stable nucleic acid; therefore, its contribution in improving the efficiency of delivery to the heart is more significant. Since this delivery method utilizes the oscillation and collapse of NBs in response to ultrasound irradiation, it was thought that the delivery effect was enhanced only in the area exposed to ultrasound, the heart tissues. Previous studies have also suggested that the combination of ultrasound and intravascularly administered NBs has little effect on delivery to areas that are not irradiated with

Table 2. Physical Properties of R8-PMO-Loaded NBs

	particle size (nm)		zeta potential (mV)	
DPPC/DPPG/PEG	R8-PMO (−)	R8-PMO (+)	R8-PMO (−)	R8-PMO (+)
94:0:6	648.1 ± 73.3	615.7 ± 80.2	−0.03 ± 0.27	0.05 ± 0.16
0:94:6	594.6 ± 82.6	521.9 ± 60.1	−0.45 ± 0.45	−0.63 ± 0.60

https://doi.org/10.1021/acsomega.4c10896
ACS Omega 2025, 10, 9639−9648

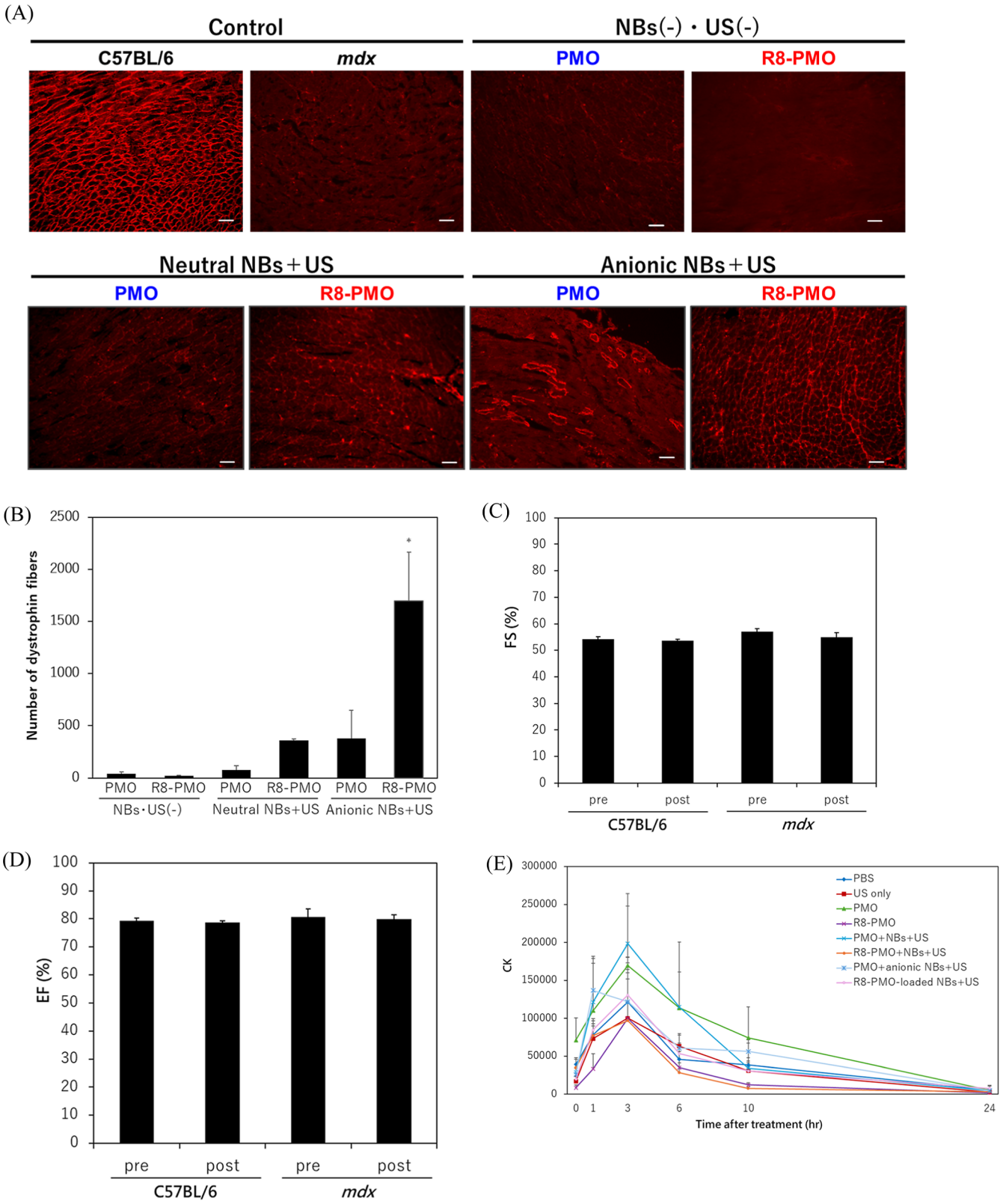

Figure 4. Restoration of dystrophin expression in the cardiac tissue of mdx mice after the PMO transfection with R8-PMO-loaded NBs and ultrasound. PMO (100 μg) and NBs (140 μg) were injected into the tail vein and the heart was exposed to ultrasound (frequency, 1 MHz; duty, 50%; intensity, 2 W/cm^2; time, 1 min). Dystrophin expression was detected by staining with NCL-DYS2 2 weeks after intravenous injection of PMO. (A) Cardiac tissue of normal C57BL/6, *mdx*, and *mdx* mice treated with PMO. Scale bar: 50 μm. (B) Quantitative evaluation of total dystrophin-positive fibers in the cardiac tissue section. The bars show the mean and SD (n = 4). * indicates $P < 0.01$ using a two-way ANOVA with Tukey's posthoc test. Cardiac function was measured using echocardiography before and after intravenous injection of NBs with ultrasound. Cardiac function is represented by (C) fractional shortening (FS) and (D) ejection fraction (EF). (E) Serum creatine kinase (CK) levels were measured before and 1, 3, 6, 10, and 24 h after the intravenous injection of PMO or R8-PMO with NBs and ultrasound.

https://doi.org/10.1021/acsomega.4c10896
ACS Omega 2025, 10, 9639−9648

ultrasound.[18,49] In this study, the CPP-bound PMO released from the surface of NBs by ultrasound could circulate from the heart to other tissues and affect their cells. However, as shown in Figure 4A, no dystrophin expression was observed in the group treated with R8-PMO alone, suggesting that the dosage used in this study had little effect on other tissues. In the future, it is essential to evaluate the effects of R8-PMO on other organs, including the side effects, when considering the administration conditions for developing cardiac therapy of muscular dystrophy. Although the exon skipping efficiency was not evaluated in this study, we assessed the induction of exon skipping and restoration of dystrophin expression following the transfection of PMO using a combination of NBs and ultrasound in previous reports.[23,31] Further detailed evaluations, including exon skipping efficiency, the duration of the effects, and toxicity assessment, are required to verify the efficacy of the PMO delivery to the heart by our method in the treatment of DMD. Repeated administration is likely required, as is the case with currently approved drugs. Therefore, the ability to safely deliver PMO without adversely affecting cardiac function is valuable for DMD treatment. Because we used relatively young *mdx* mice (5−6 weeks old) in this study, there were no significant differences in cardiac function from normal mice either before or after treatment. Therefore, further studies involving older *mdx* mice are warranted. In recent years, exon skipping by using antisense oligonucleotides is one of the most promising therapeutic techniques for DMD. The first PMO-based exon-skipping drug for treating DMD received approval from the US Food and Drug Administration (FDA) in 2016. This PMO-based drug, eteplirsen, showed limited dystrophin restoration in skeletal muscles.[50] However, there has been no evidence of significant eteplirsen uptake or activity in the heart.[51] Recently, conjugating PMOs with peptides or antibody fragments has been developed and reported to be an effective treatment in heart.[48,52,53] The combination of ultrasound and NBs may be also useful in enhancing the delivery effect of these conjugated PMOs. Furthermore, each of skeletal, myocardial, and respiratory muscles can be easily targeted by changing the ultrasound irradiation site. This is a major advantage of ultrasound-mediated delivery in the treatment for DMD, a progressive disease. Indeed, in advanced stages of DMD, injury to the diaphragm can be as severe as myocardial damage, leading to respiratory failure. Our method was useful for treating the diaphragm by changing only the position of the ultrasound probe (Figure S3). The stable NBs developed in this study could be used not only for PMO, but also for other nucleic acids, although some modifications to the nucleic acid are necessary. In recent years, genome-editing tools have been developed with the advantage of longer-lasting efficacy compared to PMO treatment.[54,55] Combined with the technologies, this method is expected to contribute to the development of effective therapies for DMD.

5. CONCLUSION

In this study, we developed stable NBs containing anionic lipids. The gas encapsulated in these NBs can be retained in vivo for a long period, which is expected to improve its effectiveness as both an ultrasound contrast agent and as a gene and nucleic acid delivery tool. It was also revealed that the cationic molecule, R8-PMO could be loaded onto its surface, indicating its potential as a new nucleic acid delivery tool to target cardiac dysfunction via systemic administration. Although further detailed analysis of the therapeutic effects and the possibility of repeated administration should be explored, this work has provided the basis for a methodology that enables efficient PMO delivery to the myocardium and diaphragm, which is considered difficult. It is also expected that other cationic molecules will be loaded onto the surface of NBs or that these NBs will be applied to the treatment of other diseases via systemic administration.

■ ASSOCIATED CONTENT

Supporting Information

The Supporting Information is available free of charge at https://pubs.acs.org/doi/10.1021/acsomega.4c10896.

Size distribution of NBs containing anionic lipids (0−94 mol %) or loading R8-PMO by Original DLS data. Restoration of dystrophin expression in the diaphragm of *mdx* mice after the PMO delivery with R8-PMO-loaded NBs and ultrasound (PDF)

■ AUTHOR INFORMATION

Corresponding Author

Yoichi Negishi − *Department of Drug Delivery and Molecular Biopharmaceutics, School of Pharmacy, Tokyo University of Pharmacy and Life Sciences, Hachioji, Tokyo 192-0392, Japan*; orcid.org/0000-0003-4364-8694; Email: negishi@toyaku.ac.jp

Authors

Yoko Endo-Takahashi − *Department of Drug Delivery and Molecular Biopharmaceutics, School of Pharmacy, Tokyo University of Pharmacy and Life Sciences, Hachioji, Tokyo 192-0392, Japan*; orcid.org/0000-0002-6881-6044

Akane Sakurai − *Department of Drug Delivery and Molecular Biopharmaceutics, School of Pharmacy, Tokyo University of Pharmacy and Life Sciences, Hachioji, Tokyo 192-0392, Japan*

Yukiko Oguri − *Department of Drug Delivery and Molecular Biopharmaceutics, School of Pharmacy, Tokyo University of Pharmacy and Life Sciences, Hachioji, Tokyo 192-0392, Japan*

Fumihiko Katagiri − *Department of Clinical Biochemistry, School of Pharmacy, Tokyo University of Pharmacy and Life Sciences, Hachioji, Tokyo 192-0392, Japan*

Saki Akiyama − *Department of Drug Delivery and Molecular Biopharmaceutics, School of Pharmacy, Tokyo University of Pharmacy and Life Sciences, Hachioji, Tokyo 192-0392, Japan*

Sanae Sashida − *Department of Drug Delivery and Molecular Biopharmaceutics, School of Pharmacy, Tokyo University of Pharmacy and Life Sciences, Hachioji, Tokyo 192-0392, Japan*

Taiki Yamaguchi − *Department of Drug Delivery and Molecular Biopharmaceutics, School of Pharmacy, Tokyo University of Pharmacy and Life Sciences, Hachioji, Tokyo 192-0392, Japan*; orcid.org/0009-0003-4453-061X

Tetsuro Marunouchi − *Department of Molecular and Cellular Pharmacology, School of Pharmacy, Tokyo University of Pharmacy and Life Sciences, Hachioji, Tokyo 192-0392, Japan*

Ryo Suzuki − *Laboratory of Drug and Gene Delivery Research, Faculty of Pharmaceutical Sciences, Teikyo*

https://doi.org/10.1021/acsomega.4c10896
ACS Omega 2025, 10, 9639−9648

University, Itabashi-ku, Tokyo 173-8605, Japan; orcid.org/0000-0001-6614-4486

Kazuo Maruyama − *Laboratory of Theranostics, Faculty of Pharmaceutical Sciences, Teikyo University, Itabashi-ku, Tokyo 173-8605, Japan*

Kouichi Tanonaka − *Department of Molecular and Cellular Pharmacology, School of Pharmacy, Tokyo University of Pharmacy and Life Sciences, Hachioji, Tokyo 192-0392, Japan*

Motoyoshi Nomizu − *Department of Clinical Biochemistry, School of Pharmacy, Tokyo University of Pharmacy and Life Sciences, Hachioji, Tokyo 192-0392, Japan;* orcid.org/0000-0002-2264-2907

Complete contact information is available at: https://pubs.acs.org/10.1021/acsomega.4c10896

Author Contributions

#Yoko Endo-Takahashi, Akane Sakurai and Yukiko Oguri are contributed equally to this work. Yoko Endo-Takahashi: Writing−original draft, Writing−review and editing, Visualization, Validation, Methodology, Investigation, Data curation, Formal analysis, Conceptualization. Akane Sakurai: Investigation, Data curation. Yukiko Oguri: Investigation, Data curation. Fumihiko Katagiri: Writing−review and editing, Methodology, Resources. Saki Akiyama: Investigation, Data curation. Sanae Sashida: Investigation, Data curation. Taiki Yamaguchi: Writing−review and editing, Investigation, Data curation, Formal analysis. Tetsuro Marunouchi: Writing−review and editing, Methodology, Investigation. Ryo Suzuki: Writing−review and editing, Supervision. Kazuo Maruyama: Writing−review and editing, Supervision. Kouichi Tanonaka: Writing−review and editing, Supervision. Motoyoshi Nomizu: Writing−review and editing, Supervision. Yoichi Negishi: Writing−review and editing, Validation, Methodology, Data curation, Conceptualization, Funding acquisition, Supervision.

Notes

The authors declare no competing financial interest.

■ ACKNOWLEDGMENTS

We are grateful to Taiki Kikuchi (School of Pharmacy, Tokyo University of Pharmacy and Life Sciences) for excellent technical assistance, to Prof. Katsuro Tachibana (Department of Anatomy, School of Medicine, Fukuoka University) for technical advice regarding the induction of cavitation with ultrasound, and to Yasuhiko Hayakawa and Kosho Suzuki (NEPA GENE Co., Ltd.) for technical advice regarding ultrasound exposure. This work was supported by a Grant for Industrial Technology Research (04A05010) from the New Energy and Industrial Technology Development Organization (NEDO) of Japan and JSPS KAKENHI Grant Numbers JP23300193, JP21H03843 and JP24K03314.

■ REFERENCES

(1) Unger, E. C.; Hersh, E.; Vannan, M.; McCreery, T. Gene Delivery Using Ultrasound Contrast Agents. *Echocardiography* **2001**, *18*, 355−361.

(2) Hernot, S.; Klibanov, A. L. Microbubbles in Ultrasound-Triggered Drug and Gene Delivery. *Adv. Drug Delivery Rev.* **2008**, *60*, 1153−1166.

(3) Sirsi, S. R.; Borden, M. A. Advances in Ultrasound Mediated Gene Therapy Using Microbubble Contrast Agents. *Theranostics* **2012**, *2*, 1208−1222.

(4) Wu, J.; Li, R. K. Ultrasound-Targeted Microbubble Destruction in Gene Therapy: A New Tool to Cure Human Diseases. *Genes Dis* **2017**, *4*, 64−74.

(5) Endo-Takahashi, Y.; Negishi, Y. Gene and Oligonucleotide Delivery via Micro- and Nanobubbles by Ultrasound Exposure. *Drug Metab. Pharmacokinet.* **2022**, *44*, 100445.

(6) Abuhelal, S.; Centelles, M. N.; Wright, M.; Mason, A. J.; Thanou, M. Development of Cationic Lipid LAH4-L1 SiRNA Complexes for Focused Ultrasound Enhanced Tumor Uptake. *Mol. Pharmaceutics* **2023**, *20*, 2341−2351.

(7) Koga, T.; Kida, H.; Yamasaki, Y.; Feril, L. B.; Endo, H.; Itaka, K.; Abe, H.; Tachibana, K. Intracranial Gene Delivery Mediated by Albumin-Based Nanobubbles and Low-Frequency Ultrasound. *Nanomaterials* **2024**, *14*, 285.

(8) Wang, X.; Li, F.; Zhang, J.; Guo, L.; Shang, M.; Sun, X.; Xiao, S.; Shi, D.; Meng, D.; Zhao, Y.; Jiang, C.; Li, J. A Combination of PD-L1-Targeted IL-15 MRNA Nanotherapy and Ultrasound-Targeted Microbubble Destruction for Tumor Immunotherapy. *J. Controlled Release* **2024**, *367*, 45−60.

(9) Chen, J.; Wang, B.; Wang, Y.; Radermacher, H.; Qi, J.; Momoh, J.; Lammers, T.; Shi, Y.; Rix, A.; Kiessling, F. MRNA Sonotransfection of Tumors with Polymeric Microbubbles: Co-Formulation versus Co-Administration. *Adv. Sci.* **2024**, *11*, No. e2306139.

(10) Owusu-Yaw, B. S.; Todd, N. Focused Ultrasound-Mediated Delivery of Viral Neuronal Tracers in Marmosets. *Cell Rep. Methods* **2024**, *4*, 100719.

(11) Tachibana, K.; Uchida, T.; Ogawa, K.; Yamashita, N.; Tamura, K. Induction of Cell-Membrane Porosity by Ultrasound. *Lancet* **1999**, *353*, 1409.

(12) Ogawa, K.; Tachibana, K.; Uchida, T.; Tai, T.; Yamashita, N.; Tsujita, N.; Miyauchi, R. High-Resolution Scanning Electron Microscopic Evaluation of Cell-Membrane Porosity by Ultrasound. *Med. Electron Microsc.* **2001**, *34*, 249−253.

(13) Lentacker, I.; De Cock, I.; Deckers, R.; De Smedt, S. C.; Moonen, C. T. W. Understanding Ultrasound Induced Sonoporation: Definitions and Underlying Mechanisms. *Adv. Drug Delivery Rev.* **2014**, *72*, 49−64.

(14) Man, V. H.; Truong, P. M.; Li, M. S.; Wang, J.; Van-Oanh, N.-T.; Derreumaux, P.; Nguyen, P. H. Molecular Mechanism of the Cell Membrane Pore Formation Induced by Bubble Stable Cavitation. *J. Phys. Chem. B* **2019**, *123*, 71−78.

(15) Buchanan, K. D.; Huang, S.; Kim, H.; MacDonald, R. C.; McPherson, D. D. Echogenic Liposome Compositions for Increased Retention of Ultrasound Reflectivity at Physiologic Temperature. *J. Pharm. Sci.* **2008**, *97*, 2242−2249.

(16) Huang, S. L.; Hamilton, A. J.; Nagaraj, A.; Tiukinhoy, S. D.; Klegerman, M. E.; McPherson, D. D.; Macdonald, R. C. Improving Ultrasound Reflectivity and Stability of Echogenic Liposomal Dispersions for Use as Targeted Ultrasound Contrast Agents. *J. Pharm. Sci.* **2001**, *90*, 1917−1926.

(17) Suzuki, R.; Takizawa, T.; Negishi, Y.; Hagisawa, K.; Tanaka, K.; Sawamura, K.; Utoguchi, N.; Nishioka, T.; Maruyama, K. Gene Delivery by Combination of Novel Liposomal Bubbles with Perfluoropropane and Ultrasound. *J. Controlled Release* **2007**, *117*, 130−136.

(18) Suzuki, R.; Takizawa, T.; Negishi, Y.; Utoguchi, N.; Sawamura, K.; Tanaka, K.; Namai, E.; Oda, Y.; Matsumura, Y.; Maruyama, K. Tumor Specific Ultrasound Enhanced Gene Transfer in Vivo with Novel Liposomal Bubbles. *J. Controlled Release* **2008**, *125*, 137−144.

(19) Suzuki, R.; Takizawa, T.; Negishi, Y.; Utoguchi, N.; Maruyama, K. Effective Gene Delivery with Novel Liposomal Bubbles and Ultrasonic Destruction Technology. *Int. J. Pharm.* **2008**, *354*, 49−55.

(20) Negishi, Y.; Endo, Y.; Fukuyama, T.; Suzuki, R.; Takizawa, T.; Omata, D.; Maruyama, K.; Aramaki, Y. Delivery of SiRNA into the Cytoplasm by Liposomal Bubbles and Ultrasound. *J. Controlled Release* **2008**, *132*, 124−130.

(21) Negishi, Y.; Matsuo, K.; Endo-Takahashi, Y.; Suzuki, K.; Matsuki, Y.; Takagi, N.; Suzuki, R.; Maruyama, K.; Aramaki, Y. Delivery of an Angiogenic Gene into Ischemic Muscle by Novel

Bubble Liposomes Followed by Ultrasound Exposure. *Pharm. Res.* **2011**, *28*, 712−719.
(22) Negishi, Y.; Tsunoda, Y.; Endo-Takahashi, Y.; Oda, Y.; Suzuki, R.; Maruyama, K.; Yamamoto, M.; Aramaki, Y. Local Gene Delivery System by Bubble Liposomes and Ultrasound Exposure into Joint Synovium. *J. Drug Deliv* **2011**, *2011*, 203986.
(23) Negishi, Y.; Ishii, Y.; Shiono, H.; Akiyama, S.; Sekine, S.; Kojima, T.; Mayama, S.; Kikuchi, T.; Hamano, N.; Endo-Takahashi, Y.; Suzuki, R.; Maruyama, K.; Aramaki, Y. Bubble Liposomes and Ultrasound Exposure Improve Localized Morpholino Oligomer Delivery into the Skeletal Muscles of Dystrophic Mdx Mice. *Mol. Pharmaceutics* **2014**, *11*, 1053−1061.
(24) Endo-Takahashi, Y.; Negishi, Y.; Kato, Y.; Suzuki, R.; Maruyama, K.; Aramaki, Y. Efficient SiRNA Delivery Using Novel SiRNA-Loaded Bubble Liposomes and Ultrasound. *Int. J. Pharm.* **2012**, *422*, 504−509.
(25) Negishi, Y.; Endo-Takahashi, Y.; Matsuki, Y.; Kato, Y.; Takagi, N.; Suzuki, R.; Maruyama, K.; Aramaki, Y. Systemic Delivery Systems of Angiogenic Gene by Novel Bubble Liposomes Containing Cationic Lipid and Ultrasound Exposure. *Mol. Pharmaceutics* **2012**, *9*, 1834−1840.
(26) Endo-Takahashi, Y.; Negishi, Y.; Nakamura, A.; Suzuki, D.; Ukai, S.; Sugimoto, K.; Moriyasu, F.; Takagi, N.; Suzuki, R.; Maruyama, K.; Aramaki, Y. PDNA-Loaded Bubble Liposomes as Potential Ultrasound Imaging and Gene Delivery Agents. *Biomaterials* **2013**, *34*, 2807−2813.
(27) Endo-Takahashi, Y.; Negishi, Y.; Nakamura, A.; Ukai, S.; Ooaku, K.; Oda, Y.; Sugimoto, K.; Moriyasu, F.; Takagi, N.; Suzuki, R.; Maruyama, K.; Aramaki, Y. Systemic Delivery of MiR-126 by MiRNA-Loaded Bubble Liposomes for the Treatment of Hindlimb Ischemia. *Sci. Rep.* **2014**, *4*, 3883.
(28) Sax, N.; Kodama, T. Optimization of Acoustic Liposomes for Improved in Vitro and in Vivo Stability. *Pharm. Res.* **2013**, *30*, 218.
(29) Hoffman, E. P.; Brown, R. H.; Kunkel, L. M. Dystrophin: The Protein Product of the Duchenne Muscular Dystrophy Locus. *Cell* **1987**, *51*, 919−928.
(30) Sekine, S.; Mayama, S.; Nishijima, N.; Kojima, T.; Endo-Takahashi, Y.; Ishii, Y.; Shiono, H.; Akiyama, S.; Sakurai, A.; Sashida, S.; Hamano, N.; Tada, R.; Suzuki, R.; Maruyama, K.; Negishi, Y. Development of a Gene and Nucleic Acid Delivery System for Skeletal Muscle Administration via Limb Perfusion Using Nanobubbles and Ultrasound. *Pharmaceutics* **2023**, *15*, 1665.
(31) Negishi, Y.; Ishii, Y.; Nirasawa, K.; Sasaki, E.; Endo-Takahashi, Y.; Suzuki, R.; Maruyama, K. PMO Delivery System Using Bubble Liposomes and Ultrasound Exposure for Duchenne Muscular Dystrophy Treatment. *Methods Mol. Biol.* **2018**, *1687*, 185−192.
(32) Roberts, T. C.; Langer, R.; Wood, M. J. A. Advances in Oligonucleotide Drug Delivery. *Nat. Rev. Drug Discovery* **2020**, *19*, 673−694.
(33) Shah, M. N. A.; Yokota, T. Cardiac Therapies for Duchenne Muscular Dystrophy. *Ther. Adv. Neurol. Disord.* **2023**, *16*, 17562864231182934.
(34) Futaki, S.; Suzuki, T.; Ohashi, W.; Yagami, T.; Tanaka, S.; Ueda, K.; Sugiura, Y. Arginine-Rich Peptides. An Abundant Source of Membrane-Permeable Peptides Having Potential as Carriers for Intracellular Protein Delivery. *J. Biol. Chem.* **2001**, *276*, 5836−5840.
(35) Wender, P. A.; Mitchell, D. J.; Pattabiraman, K.; Pelkey, E. T.; Steinman, L.; Rothbard, J. B. The Design, Synthesis, and Evaluation of Molecules That Enable or Enhance Cellular Uptake: Peptoid Molecular Transporters. *Proc. Natl. Acad. Sci. U.S.A.* **2000**, *97*, 13003−13008.
(36) Endo-Takahashi, Y.; Kurokawa, R.; Sato, K.; Takizawa, N.; Katagiri, F.; Hamano, N.; Suzuki, R.; Maruyama, K.; Nomizu, M.; Takagi, N.; Negishi, Y. Ternary Complexes of Pdna, Neuron-Binding Peptide, and Pegylated Polyethyleneimine for Brain Delivery with Nano-Bubbles and Ultrasound. *Pharmaceutics* **2021**, *13*, 1003.
(37) Fiske, C. H.; Subbarow, Y. THE COLORIMETRIC DETERMINATION OF PHOSPHORUS. *J. Biol. Chem.* **1925**, *66*, 375−400.
(38) Yin, H.; Saleh, A. F.; Betts, C.; Camelliti, P.; Seow, Y.; Ashraf, S.; Arzumanov, A.; Hammond, S.; Merritt, T.; Gait, M. J.; Wood, M. J. A. Pip5 Transduction Peptides Direct High Efficiency Oligonucleotide-Mediated Dystrophin Exon Skipping in Heart and Phenotypic Correction in Mdx Mice. *Mol. Ther.* **2011**, *19*, 1295−1303.
(39) Marunouchi, T.; Yano, E.; Tanonaka, K. Effects of Cardiosphere-Derived Cell Transplantation on Cardiac Mitochondrial Oxygen Consumption after Myocardial Infarction in Rats. *Biomed. Pharmacother.* **2018**, *108*, 883−892.
(40) Zheng, R.; Yin, T.; Wang, P.; Zheng, R.; Zheng, B.; Cheng, D.; Zhang, X.; Shuai, X. T. Nanobubbles for Enhanced Ultrasound Imaging of Tumors. *Int. J. Nanomedicine* **2012**, *7*, 895−904.
(41) Lewis, R. N. A. H.; Zhang, Y. P.; McElhaney, R. N. Calorimetric and Spectroscopic Studies of the Phase Behavior and Organization of Lipid Bilayer Model Membranes Composed of Binary Mixtures of Dimyristoylphosphatidylcholine and Dimyristoylphosphatidylglycerol. *Biochim. Biophys. Acta Biomembr.* **2005**, *1668*, 203.
(42) Unga, J.; Omata, D.; Kudo, N.; Ueno, S.; Munakata, L.; Shima, T.; Suzuki, R.; Maruyama, K. Development and Evaluation of Stability and Ultrasound Response of DSPC-DPSG-Based Freeze-Dried Microbubbles. *J. Liposome Res.* **2019**, *29*, 368−374.
(43) Maruyama, T.; Sugii, M.; Omata, D.; Unga, J.; Shima, T.; Munakata, L.; Kageyama, S.; Hagiwara, F.; Suzuki, Y.; Maruyama, K.; Suzuki, R. Effect of Lipid Shell Composition in DSPG-Based Microbubbles on Blood Flow Imaging with Ultrasonography. *Int. J. Pharm.* **2020**, *590*, 119886.
(44) Summerton, J.; Weller, D. Morpholino Antisense Oligomers: Design, Preparation, and Properties. *Antisense Nucleic Acid Drug Dev* **1997**, *7*, 187−195.
(45) Amantana, A.; Iversen, P. L. Pharmacokinetics and Biodistribution of Phosphorodiamidate Morpholino Antisense Oligomers. *Curr. Opin. Pharmacol.* **2005**, *5*, 550−555.
(46) Wu, R. P.; Youngblood, D. S.; Hassinger, J. N.; Lovejoy, C. E.; Nelson, M. H.; Iversen, P. L.; Moulton, H. M. Cell-Penetrating Peptides as Transporters for Morpholino Oligomers: Effects of Amino Acid Composition on Intracellular Delivery and Cytotoxicity. *Nucleic Acids Res.* **2007**, *35*, 5182−5191.
(47) Said Hassane, F.; Saleh, A. F.; Abes, R.; Gait, M. J.; Lebleu, B. Cell Penetrating Peptides: Overview and Applications to the Delivery of Oligonucleotides. *Cell. Mol. Life Sci.* **2010**, *67*, 715−726.
(48) Gan, L.; Wu, L. C. L.; Wood, J. A.; Yao, M.; Treleaven, C. M.; Estrella, N. L.; Wentworth, B. M.; Hanson, G. J.; Passini, M. A. A Cell-Penetrating Peptide Enhances Delivery and Efficacy of Phosphorodiamidate Morpholino Oligomers in Mdx Mice. *Mol. Ther Nucleic Acids* **2022**, *30*, 17−27.
(49) Negishi, Y.; Yamane, M.; Kurihara, N.; Endo-Takahashi, Y.; Sashida, S.; Takagi, N.; Suzuki, R.; Maruyama, K. Enhancement of Blood−Brain Barrier Permeability and Delivery of Antisense Oligonucleotides or Plasmid DNA to the Brain by the Combination of Bubble Liposomes and High-Intensity Focused Ultrasound. *Pharmaceutics* **2015**, *7*, 344−362.
(50) Mendell, J. R.; Goemans, N.; Lowes, L. P.; Alfano, L. N.; Berry, K.; Shao, J.; Kaye, E. M.; Mercuri, E. Longitudinal Effect of Eteplirsen versus Historical Control on Ambulation in Duchenne Muscular Dystrophy. *Ann. Neurol.* **2016**, *79*, 257.
(51) Lim, K. R. Q.; Maruyama, R.; Yokota, T. Eteplirsen in the Treatment of Duchenne Muscular Dystrophy. *Drug Des Devel Ther* **2017**, *11*, 533−545.
(52) Nguyen, Q.; Yokota, T. Antisense Oligonucleotides for the Treatment of Cardiomyopathy in Duchenne Muscular Dystrophy. *Am. J. Transl. Res.* **2019**, *11*, 1202−1218.
(53) Desjardins, C. A.; Yao, M.; Hall, J.; O'Donnell, E.; Venkatesan, R.; Spring, S.; Wen, A.; Hsia, N.; Shen, P.; Russo, R.; Lan, B.; Picariello, T.; Tang, K.; Weeden, T.; Zanotti, S.; Subramanian, R.; Ibraghimov-Beskrovnaya, O. NAR Breakthrough Article Enhanced Exon Skipping and Prolonged Dystrophin Restoration Achieved by TfR1-Targeted Delivery of Antisense Oligonucleotide Using FORCE Conjugation in Mdx Mice. *Nucleic Acids Res.* **2022**, *50*, 11401−11414.

https://doi.org/10.1021/acsomega.4c10896
ACS Omega 2025, 10, 9639−9648

(54) Kenjo, E.; Hozumi, H.; Makita, Y.; Iwabuchi, K. A.; Fujimoto, N.; Matsumoto, S.; Kimura, M.; Amano, Y.; Ifuku, M.; Naoe, Y.; Inukai, N.; Hotta, A. Low Immunogenicity of LNP Allows Repeated Administrations of CRISPR-Cas9MRNA into Skeletal Muscle in Mice. *Nat. Commun.* **2021**, *12*, 7101.
(55) Happi Mbakam, C.; Lamothe, G.; Tremblay, G.; Tremblay, J. P. CRISPR-Cas9 Gene Therapy for Duchenne Muscular Dystrophy. *Neurotherapeutics* **2022**, *19*, 931−941.

https://doi.org/10.1021/acsomega.4c10896
ACS Omega 2025, 10, 9639−9648